Journal of Design Against Fatigue, Vol. 1, No. 3, (2023) 12-18

Journal of Design Against Fatigue
https://minerva-aset.com/JDAF

Experimental and Numerical Fracture Toughness Evaluation of Spiral Seam Weld of API X65 Steel

Ali Farrahi[1,*], Seyyed Hojjat Hashemi[2]

[1]*Department of Applied Mechanics, Faculty of Mechanical Engineering, K.N.Toosi University of Technology, Tehran, Iran.*
[2]*Department of Mechanical Engineering, University of Birjand, Birjand, Iran.*

P A P E R I N F O

Paper history:
Received 25 September 2023
Received in revised form 29 September 2023
Accepted 30 September 2023

Keywords:
Fracture toughness
API X65 steel
Spiral seam weld
SENT
GTN Model

A B S T R A C T

In this research fracture toughness of spiral seam weld of API X65 is measured through the ASTM E1820 standard recommendations. According to thin-wall pipe of API X65 in this research, specimen sizes could not satisfy the plain strain condition of ASTM E399 therefore, indirect method is accomplished by evaluating the crack tip opening displacement. According to the nature of welding procedure and inhomogeneous probable defects in the different regions of seam weld, δ-R curve with multi-specimen technique of single-edge notched bend (SENB) specimens is applied for test procedure in this research. The measured CTOD and K_{1C} are 0.23 mm and 265 $MPam^{3/2}$ respectively. Furthermore, Three-dimensional finite element method numerical evaluation of crack propagation with GTN model has been performed. Good agreement with the other researches was observed for CTOD and fracture toughness of tested material. The difference was about 10 percent.

***doi**:*

1. INTRODUCTION

Steel pipelines are one of the most important equipment for gas transportation network. Therefore, a complete investigation should be accomplished [1]. High Strength Low Alloys (HSLA) steels offer the best possible combination of strength and toughness, with their thermo-mechanical controlling process (TMCP) [2,3]. In general, flexible production process leads manufacturers to spiral seam weld pipes[4]. According to the nature of welding process, microstructure alteration, probable flaws and residual stresses can degrade buckling strength, brittle fracture strength, and fatigue life [5,6]. Fracture toughness has its importance for structural integrity assessment, failure assessment diagram (FAD) and fitness-for service (FFS) assessment of flaws that are found in pipelines during operation [7-9]. Several ASTM standard codes [10,11] are constructed for fracture toughness measurement as K_{IC} , J-integral or CTOD (δ). Furthermore, two techniques of multiple-specimens and single-specimen are developed in ASTM E1820 for constructing R-curves. In single-specimen technique an unloading reloading compliance method is applied to construct load-displacement diagram[12,13]. However, in multi-specimen technique various specimens with the same configuration are applied. In compliance method the measured quantities are only from a specified location of material and considering the nature of welding procedure and inhomogeneous probable defects, the multi-specimen technique is preferred. In this technique, specimens are extracted from different locations of structure. So an average of fracture toughness of the material would be measured and pronounced as the toughness property of the structure [14]. According to ASTM and material characteristics of seam weld, the multiple-specimens technique using single edge notched bending configuration is used to evaluate the fracture toughness [15]. Fracture toughness of seem welded API X65 was assessed at low temperature [16]. Compliance method using single specimen technique was used for measuring the KIC of API X65 [17]. To demonstrate the effect of residual stresses and heat treatment (as stress relaxation) on fracture toughness of seam weld of API X65 CTOD is reported and compared [5]. Also length of notch (as a geometrical constraint) effect is discussed for girth weld of API X65 through R-curves with different aspect ratios (a0/W) [18]. Furthermore, CTOD is measured to evaluate FADs of API X65 [7]. On the other hand, the GTN model is used for evaluating of fracture behavior of ductile materials based on void nucleation, growth and coalescence [19,20]. So, three-dimensional crack propagation based on CTOD [21] and GTN model [22], finite element numerical analysis of fracture behavior of material is performed.

*Corresponding Author Email: ***farrahi@ymail.com, afarrahi@mail.kntu.ac.ir*** (Dr Ali Farrahi)

Cite this article as: A.Farrahi, S.H.Hashemi, Experimental and Numerical Fracture Toughness Evaluation of Spiral Seam Weld of API X65 Steel, ***Journal of Design Against Fatigue,*** Vol. 1, No. 3, (2023)

In this research, SENB configuration with multiple-specimens technique is utilized to evaluate the fracture toughness of seam weld of API X65 with spiral shape. Also, three-dimensional finite element method with GTN damage model is used to compare with experimental results. Multiple-specimen technique has not been employed to investigate the spiral seam weld and this is the novelty of this paper. Furthermore, three-dimensional FEM on SENB specimens also implemented for this investigation. According to the results, good agreement between experimental and numerical results is observed. Moreover, appropriate correlation between present results and the other researches on API X65 grade is presented.

2. MATERIAL PROPERTIES AND EXPERIMENTAL PROCEDURE

2.1. Material Properties

Chemical composition and material properties of seam weld of API X65 steel is given in TABLE 1 and TABLE 2 respectively, also the geometrical characteristics of pipe and seam weld is given in TABLE 3.

TABLE 1: Chemical composition of fusion zone and target values specified by API 5L [23].

Element	Weight% in FZ	Maximum (API 5L X65)
Fe	Base	-
Carbon Equivalent (CE)	0.260	0.430
Carbon	0.73	0.220
Manganese	1.370	1.450
Phosphor	0.010	0.025
Sulphur	0.003	0.015
Titanium	0.008	0.060

TABLE 2: Measured mechanical properties of fusion zone X65 pipeline in transverse direction of pipe [24].

Mechanical property	Value
Young's modulus (GPa)	253
Yield Strength (MPa)	548
Ultimate Tensile Strength (MPa)	624
YS/UTS	0.88
Elongation (%)	17

TABLE 3: Geometrical characteristics of API X65 tested pipe.

Characteristic	Value (Shape)
Outer Diameter (mm)	1219
Wall Thickness (mm)	14.3
OD/WT	85
Groove Shape	X
Welding Technique	Spiral SAW
Seam Angle (°)	22

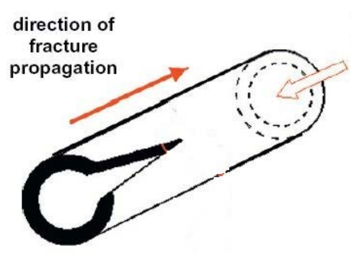

Figure 1: Direction of fracture propagation of gas transportation pipelines [23].

Gas transportation pipelines are thin-wall pipes. Consequently, in this type of pipes the hoop stress (in transverse direction) is the maximum one. Therefore, the fracture propagation according to Figure 1 is in the axial direction of pipe (perpendicular to the maximum stress).

2.2. Specimen Preparation

ASTM E399 code is developed for plane-strain fracture toughness of metallic materials. According to this code, K_{IC} is measured in a direct method. Hence, ($B \geq 2.5(\frac{K_{IC}}{\sigma_{YS}})^2$) the least thickness of three point bending test specimen of researched material should be 60 centimeters. However, the relevant dimension of pipe is 14.3 mm, so another method is developed to measure fracture toughness which is appropriate for materials with ductile behavior. J-integral or CTOD (δ) are used to describe the resistance curve for ductile fracture.
The most comprehensive standard code to evaluate J-integral or CTOD is ASTM E1820. J_{IC} and CTOD evaluation are developed recent decades and some modified upper bounds of R-curves and equations are defined for measurement of fracture toughness of industrial structures which have limitations to provide geometrical conditions of standard specimens [7]. According to ASTM standard and material characteristics of seam weld and pipe configuration limitations of wall thickness and curvature, single edge notched bending (SENB) configuration is used to evaluate the fracture toughness[15]. Therefore, SENB specimens with 60 mm length, 10 mm width, 10 mm thickness and 5.05 mm initial crack length have been extracted from the pipe. As noted the fracture propagation is in the axial direction, so the test samples machined from the mid-thickness in the transverse direction of pipe. The notch direction is in the T-L direction according to the definition of ASTM E1820 [11]. Also Figure 2 illustrates the location and direction of test specimens in the pipe.

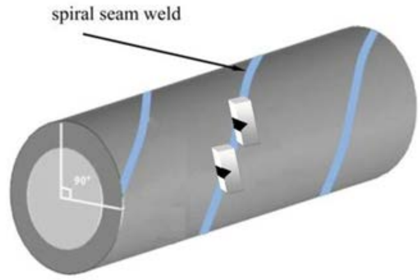

Figure 2: Location and direction of test specimens.

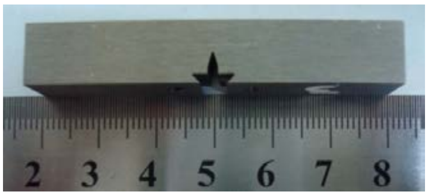

Figure 3: Test specimen machined at the middle of wall thickness.

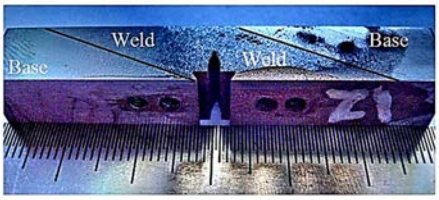

Figure 4: Notch location and corresponding crack propagation through the spiral fusion zone.

The three points bending test specimen is showed in Figure 3. The integral knife edges for clip gage are located through the sides of the notch. The notch and its corresponding crack propagation should be in the fusion zone, so macro-etch has been accomplished for assurance of crack location, see Figure 4.

2.3. Experimental Procedure and Analysis

The 600 KN Zwick tensile test machine has been utilized for experiments. According to Figure 5, three points bending test fixture has been designed and manufactured according to recommendations of [11].

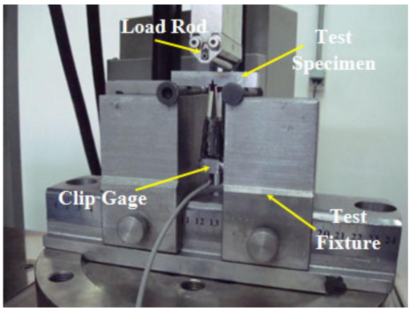

Figure 5: three points bending test fixture of API X65 steel.

TABLE 4: applied displacements to different specimens.

Specimen number	Displacement (mm)
1	2.20
2	5.73
3	2.90
4	1.41
5	2.02
6	2.72

Figure 6: Specimens with different applied displacements for multiple-specimens technique.

As noted, K_{IC} cannot be measured with direct method (ASTM E399) in the case of this research. Therefore, δ-R curve, as an indirect method, was used for evaluation of fracture toughness. In multiple-specimens technique for three points bending test, at least five test specimens with the same geometrical dimensions and initial crack length is needed. The same specimens are loaded to different displacements and the data should be located in the valid region of R-curve to measure the parameter [11]. TABLE 4 demonstrates the different displacements of same specimens and Figure 6 shows the specimens with different displacements for multiple-specimens technique of δ-R curve.
The ligament should be brittle fractured after the experimental procedure to reveal the crack propagation of each specimen [11]. To determine the physical crack length, high definition macro photographs are taken from each fractured section. Each photo has been analyzed by image processing software to measure the physical crack length according to [11] with the most accuracy. TABLE 5 demonstrates the physical crack length of different specimens. According to constructed R-curve and standard requirements of ASTM E1820, the R-square of plotted trend-line of tested points which located in valid area expresses high regression and no repeated test in needed.

TABLE 5: Physical crack length of different specimens with different applied displacements.

Applied displacement (mm)	Physical crack length (mm)
2.20	0.54
5.73	2.12
2.90	0.72
1.41	0.27
2.02	0.29
2.72	0.88

TABLE 6: CTOD of different specimens with their corresponding crack length.

Δa (mm)	δ (mm)
0.54	0.274
2.12	0.972
0.72	0.399
0.27	0.161
0.29	0.236
0.88	0.403

To measure fracture toughness with CTOD, within the test procedure crack mouth opening displacement (CMOD) should be measured and recorded. So a clip gage having strain gages on each blade, is needed to measure the CMOD. For continuous recording of CMOD, P3 Strain indicator of Vishay-Micro measurement is applied. According to [11], CTOD is determined by eq. (1):

$$= \frac{K^2(1-\nu^2)}{2\sigma_{YS}E} + \frac{\left[r_p(W-a)+\Delta a\right]V_{pl}}{\left[r_p(W-a)+a+z\right]} \quad (1)$$

In this equation, K is stress intensity factor, σ_{YS} is yield strength, Δa is physical crack length, z is knife edge height (for integral knife edge is zero), r_p is plastic rotation factor (for 3PB specimen is 0.44) and V_{pl} is plastic component of CMOD at the point of evaluation on the load-displacement curve. The stress intensity factor is measured by eq. (2) [11]:

$$K = \left(\frac{P.S}{BW^{\frac{3}{2}}}\right).f\left(\frac{a}{W}\right) \quad (2)$$

In this equation, P is the final load of test procedure, S, B and W are span, thickness and width of specimen respectively, and f(a/W) is the shape factor which quantity is determined by eq. (3):

$$f\left(\frac{a}{W}\right) = \frac{3(\frac{a}{W})^{1/2}[1.99-(\frac{a}{W})(1-\frac{a}{W})(2.15-3.93\left(\frac{a}{W}\right)+2.7\left(\frac{a}{W}\right)^2)]}{2(1+\frac{2a}{W})(1-\frac{a}{W})^{3/2}} \quad (3)$$

These equations are applied for each test data to determine δ. TABLE 6 demonstrates the δ of different test specimens with their corresponding physical measured crack length. Data of Table 6 are applied to construct the δ-R curve.

3. NUMERICAL SIMULATION

Three-dimensional finite element analysis of crack nucleation and propagation is modeled with micro mechanical Gurson–Tvergaard–Needleman (GTN) damage model. For the simulation of ductile fracture using GTN model, different material properties called Gurson parameters have to be determined experimentally. This model describes the growth and coalescence of voids which are nucleated at particles or even presented initially in a porous material [12]. TABLE 7 expresses the weld material Gurson parameters [23]. So, related elastic-plastic and porous plastic properties of weld material were defined to model the damage and corresponding crack propagation according to void volume fraction (VVF). It should be noted, the weld metal properties was assigned to the whole model.

According to the symmetric configuration, half of geometry was modeled with symmetric defined plane as the crack growth plane. Also, quadratic brick 3D stress elements (C3D20R) were selected for meshing and several partitions were defined to optimize the mesh distribution based on geometry, load and boundary conditions, see Figure 7. Moreover, mesh sensitivity was performed on different paths to assure the mesh density. Three different parts of main specimen, support and loading lever were modeled. The two last parts were modeled as rigid bodies. Furthermore, stress contours before and after crack propagation are illustrated on Figure 8.

TABLE 7: Measured Gurson parameters.

Parameter	Obtained value
q_1	1.5
q_2	1
Void nucleation	
ε_N	0.3
S_N	0.1
f_N	0.004
Void growth/coalescence	
f_0	$1.226\text{x}10^{-4}$
f_c	0.012
f_f	0.27

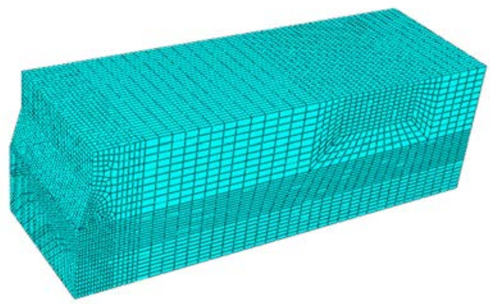

Figure 7: Mesh distribution on model with symmetric configuration.

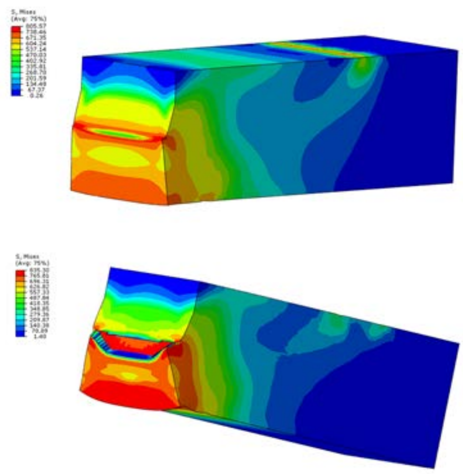

Figure 8: Von-Mises stress contour before (top) and after (bottom) crack propagation.

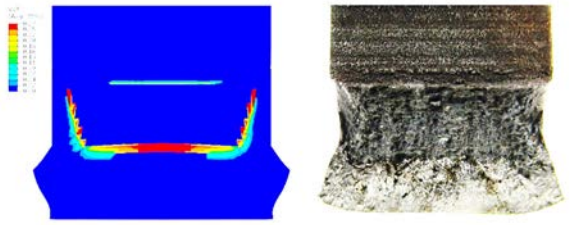

Figure 9: Fractured surface comparison of tested (right) and modeled (left) specimens.

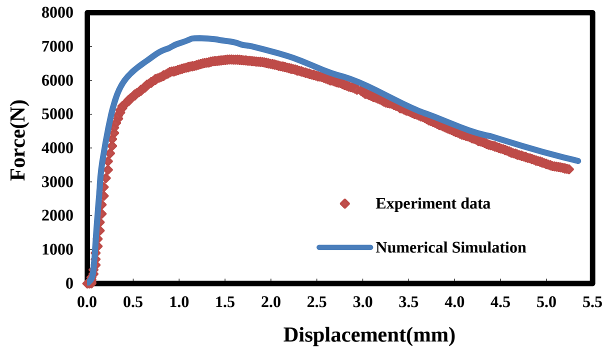

Figure 10: Comparison of experimental and numerical data of 3PB of weld material.

Physical comparison between fracture surface of experiments and numerical model with ABAQUS is illustrated in Figure 9. It can be seen that the thumb-nail shape of crack front was in appropriate similarity with the experimental one. Hence, the reaction force vs. displacement of load probe are compared in Figure 10 which reveals good agreement between experimental and numerical results.

4. RESULTS AND DISSCUSION

The intersect of power law regression line of data and 0.2 mm exclusion line parallel to blunting line with the slope of 1.4 demonstrates the initiation of crack which is defined as the CTOD of the material. According to Figure 11, The intersection of these two lines shows 0.23 mm for CTOD of seam weld of API X65 steel. Therefore, determination of fracture toughness needs an equation to associate the CTOD with fracture toughness. Eq. (4) explains the association of CTOD and fracture toughness.

$$K_{IC} = \sqrt{m(CTOD)E'\sigma_{YS}} \qquad (4)$$

In this equation, m and E' are determined according to experiment conditions. As respects to prevail of plain strain condition in test specimens, m and E' are equal to 2 and E/(1-ν2) respectively [6,7,25]. The measured CTOD and corresponding K_{IC} of seam weld of API X65 steel are 0.23 mm and 265 MPa√m respectively.

As noted, two kinds of R-curves could be obtained for toughness evaluation, but J-R curve could not be determined due to the small sizes of specimens [26] and data of diagram would not seat in the valid region and the fracture toughness would be over-evaluated. Table 8 is formed to validate the measured CTOD and corresponding K_{IC}. Through this table the geometrical and mechanical characteristics of seam weld of API X65 steel in various researches are compared. As a result the measured values show good agreement with corresponding values in other references. It should be noted, the fracture characteristics values could be affected by geometrical characteristics (WT/OD) due to manufacturing process, in addition with chemical composition and mechanical properties of material.

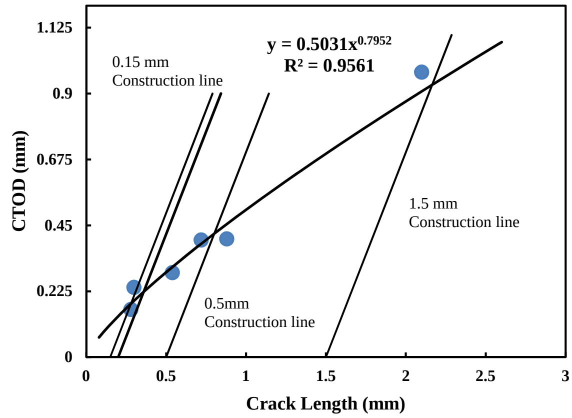

Figure 11: Constructed δ-R curve of weld of APL X65.

TABLE 8: comparison of CTOD and K_{IC} of seam weld of API X65 steel according to mechanical and geometrical characteristics.

Ref.	[5]	[7]	[7] Long. Crack	[16]	Present research
OD (mm)	416	762	762	970	1219
WT (mm)	17.5	17.5	17.5	27.8	14.3
WT/OD	0.04	0.02	0.02	0.03	0.01
Seam Weld's Direction	Long.	Long.	Long.	Long.	Spiral
Tensile Strength (MPa)	-	681	681	650	624
CTOD (mm)	0.24	0.27	0.26	0.21	0.23
K_{IC} (MPa√m)	-	267	242	-	265

TABLE 9: Evaluated fracture characteristics of weld material of API X65.

Method	K_{IC}(MPa√m)
Experiment	265
FEM	302

The fracture characteristics of seam weld material has been analyzed with obtained numerical results and according to Table 9, the results show difference of less than 14 percent between experimental and numerical evaluations which is acceptable taking into account the limitations in the numerical analysis. Amongst the limitations is the specimen configuration; base and weld metal are both present in the specimen. On the other hand, the crack propagation will be located in the weld metal. As a result, the properties of the weld metal was assigned to the whole model. Furthermore, due to the nature of welding process, some residual stresses are present in the fusion zone and this stress field is not considered in this research. Therefore, regarding the limitations in the numerical evaluation, the comparison shows satisfying validation.

5. CONCLUSIONS

Due to thin-wall pipe of API X65 used in this research, specimen sizes could not satisfy the plain strain condition of ASTM E399, so indirect method (R-curve) was accomplished by evaluating the crack tip opening displacement.
Due to the nature of welding procedure and inhomogeneous probable defects in the different regions of seam weld, the multiple-specimens method is preferred for test procedure in this research.
The GTN model with three-dimensional finite element method was utilized to evaluate the crack initiation and propagation in weld material in order to compare with experimental data. The crack propagation pattern and reaction force were in good agreement. The thumb-nail shape of crack front was in appropriate similarity with the experimental one. Also, the reaction force of numerical model was higher than the experimental data which can be explained by the effect of residual stresses present in the specimen. However, the numerical and experimental data comparison reveals less than 14% deviation which can be accepted.
The measured CTOD and K_{IC} are compared with various researches on the same grade steel. According to the comparison, this research is the only one with spiral seam weld. Furthermore, the aspect ratio of thickness to outer diameter of the present pipe is the least among the others. However, good agreement was observed for CTOD and fracture toughness of tested material. It should be noted, The CTOD is the direct parameter which is extracted form test data and shows less difference in comparison with the K_{IC} which is calculated from CTOD and some mechanical properties which could be different in various pipes with different chemical composition and manufacturing process.

6. CONFLICTS OF INTEREST

The authors declared no potential conflicts of interest with respect to the research, authorship, and/or publication of this article.

7.REFERENCES

1. Yang, Z. Z., W. Tian, Q. R. Ma, Y. L. Li, J. K. Li, J. Z. Gao, H. B. Zhang, and Y. H. Yang. Mechanical properties of longitudinal submerged arc welded steel pipes used for gas pipeline of offshore oil. *Acta Metallurgica Sinica (English Letters)* 21, no. 2 (2008): 85-93. https://doi.org/10.1016/S1006-7191(08)60024-1
2. Ju, Jang-Bog, Jung-Suk Lee, and Jae-il Jang. Fracture toughness anisotropy in a API steel line-pipe. *Materials Letters* 61, no. 29 (2007): 5178-5180. https://doi.org/10.1016/j.matlet.2007.04.007
3. Hashemi, S. H. Strength–hardness statistical correlation in API X65 steel. *Materials Science and Engineering: A* 528, no. 3 (2011): 1648-1655. https://doi.org/10.1016/j.msea.2010.10.089
4. Kennedy, John L. Oil and gas pipeline fundamentals. 2nd ed. Pennwell Publ, Oklahoma. (1984).
5. Ju, Jang-Bog, Jung-Suk Lee, Jae-il Jang, Woo-sik Kim, and Dongil Kwon. Determination of welding residual stress distribution in API X65 pipeline using a modified magnetic Barkhausen noise method. *International Journal of Pressure Vessels and Piping* 80, no. 9 (2003): 641-646. https://doi.org/10.1016/S0308-0161(03)00131-5
6. Dowling NE, Mechanical behavior of materials, 2nd ed. Prentice Hall Publ, New Jersey, 1999.
7. Zhu, Xian-Kui, and James A. Joyce. Review of fracture toughness (G, K, J, CTOD, CTOA) testing and standardization. *Engineering fracture mechanics* 85 (2012): 1-46. https://doi.org/10.1016/j.engfracmech.2012.02.001
8. Lee, Jung-Suk, Jang-Bog Ju, Jae-il Jang, Woo-Sik Kim, and Dongil Kwon. Weld crack assessments in API X65 pipeline: failure assessment diagrams with variations in representative mechanical properties. *Materials Science and Engineering: A* 373, no. 1-2 (2004): 122-130. https://doi.org/10.1016/j.msea.2003.12.039
9. Nie, H., Ma, W., Xue, K., Ren, J., Dang, W., Wang, K., Cao, J., Yao, T. and Liang, X., 2021. A novel test method for mechanical properties of characteristic zones of girth welds. *International Journal of Pressure Vessels and Piping*, *194*, p.104533. https://doi.org/10.1016/j.ijpvp.2021.104533
10. ASTM standard E399, Standard test method for plane-strain fracture toughness of metallic materials, In: Annual book of ASTM standards, 1997.
11. ASTM standard E1820, Standard test method for measurement of fracture toughness. In: Annual book of ASTM standards , 2002.
12. Espeseth, V., Morin, D., Børvik, T., & Hopperstad, O. S. (2023). A gradient-based non-local GTN model: Explicit finite element simulation of ductile damage and fracture. *Engineering Fracture Mechanics*, 109442. https://doi.org/10.1016/j.engfracmech.2023.109442
13. Cao, Y., Chang, Q., & Zhen, Y. (2022). Numerical simulation of fracture behavior for the pipeline with girth weld under axial load. *Engineering Failure Analysis*, *136*, 106221. https://doi.org/10.1016/j.engfailanal.2022.106221
14. Maropoulos S, Ridley N, Kechagias J, Karagiannis S (2004) Fracture toughness evaluation of a H.S.L.A steel. Engng Fract Mech (71): 1695-1704. https://doi.org/10.1016/j.engfracmech.2003.08.006
15. Liu, Z., Wang, X., Miller, R. E., Hu, J., & Chen, X. (2021). Fracture toughness of thermal aged 16MND5 bainitic forging steel under varying 3D constraint conditions: an experimental study using SENT specimens. *Theoretical and Applied Fracture Mechanics*, *114*, 103025. https://doi.org/10.1016/j.tafmec.2021.103025
16. Alipour Yengejeh, E., Torun, AR., Khajedezfouli, M., Choupani. N., Fracture Toughness Assessment of Longitudinally Seam-Welded Gas Pipelines at Low Temperatures. Journal of Pipeline Systems Engineering and Practice 11, no. 4 (2020): 04020049. https://orcid.org/0000-0001-7872-6408 nchoupani@atu.edu.tr
17. Asghari V, Choupani N, Hanifi M. Experimental determination of fracture toughness of base steel and longitudinal seam weld in API X65 gas line-pipe using unloading compliance method. Modares Mechanical Engineering 16, no. 11 (2017): 284-290.

http://mme.modares.ac.ir/article-15-5885-en.html
18. Zhou, D. W. Measurement and modelling of R-curves for low-constraint specimens. *Engineering Fracture Mechanics* 78, no. 3 (2011): 605-622. https://doi.org/10.1016/j.engfracmech.2010.08.019
19. Chahboub, Yassine, and Szabolcs Szávai. Determination of GTN parameters for SENT specimen during ductile fracture. *Procedia Structural Integrity* 16 (2019): 81-88. https://doi.org/10.1016/j.prostr.2019.07.025
20. Acharyya, S., and S. Dhar. A complete GTN model for prediction of ductile failure of pipe. Journal of Materials Science 43, no. 6 (2008): 1897-1909. https://doi.org/10.1016/j.mtcomm.2022.105223
21. Zuo, Jianzheng, Xiaomin Deng, Michael A. Sutton, and Chin Shang Cheng. Three-Dimensional Crack Growth in Ductile Materials: Effect of Stress Constraint on Crack Tunneling. Journal of Pressure Vessel Technology 130, no. 3 (2008): 031401. https://doi.org/10.1016/j.engfracmech.2022.109015
22. Zhang, Yinhui, Jian Shuai, Zhiyang Lv, and Tieyao Zhang. Study on fracture behavior of pipeline girth weld based on CTOD-Am method and Gurson ductile damage model. *Theoretical and Applied Fracture Mechanics* 123 (2023): 103692. https://doi.org/10.1016/j.tafmec.2022.103692
23. Hashemi, S. H., S. Sedghi, V. Soleymani, and D. Mohammadyani. CTOA levels of welded joint in API X70 pipe steel. *Engineering Fracture Mechanics* 82 (2012): 46-59. https://doi.org/10.1016/j.engfracmech.2011.11.022
24. Rezaei yekta, M. Numerical simulation of notched specimens tensile test of API X65 with Gurson Model. MSc Thesis, Birjand University, 2010.
25. He, Min, and Fuguo Li. Modified transformation formulae between fracture toughness and CTOD of ductile metals considering pre-deformation effects. *Engineering fracture mechanics* 77, no. 14 (2010): 2763-2771. https://doi.org/10.1016/j.engfracmech.2010.06.021
26. Oh, Chang-Kyun, Yun-Jae Kim, Jong-Hyun Baek, Young-Pyo Kim, and Woosik Kim. A phenomenological model of ductile fracture for API X65 steel. *International Journal of Mechanical Sciences* 49, no. 12 (2007): 1399-1412. https://doi.org/10.1016/j.ijmecsci.2007.03.008